Received: 24 August 2017 | Revised: 20 December 2017 | Accepted: 8 January 2018

DOI: 10.1002/hbm.23974

RESEARCH ARTICLE

WILEY

Response selection codes in neurophysiological data predict conjoint effects of controlled and automatic processes during response inhibition

Witold X. Chmielewski[1] | Moritz Mückschel[1,2] | Christian Beste[1]

[1]Cognitive Neurophysiology, Department of Child and Adolescent Psychiatry, Faculty of Medicine, TU Dresden, Dresden, Germany

[2]MS Centre Dresden, Faculty of Medicine of the TU Dresden, Dresden, Germany

Correspondence
Witold X. Chmielewski, Cognitive Neurophysiology, Department of Child and Adolescent Psychiatry, TU Dresden, Schubertstrasse 42, D-01309 Dresden, Germany.
Email: witold.chmielewski@uniklinikum-dresden.de

Funding information
Deutsche Forschungsgemeinschaft (DFG), Grant/Award Number: SFB 940 project B8

Abstract

The inhibition of prepotent responses is a requirement for goal-directed behavior and several factors determine corresponding successful response inhibition processes. One factor relates to the degree of automaticity of pre-potent response tendencies and another factor relates to the degree of cognitive control that is exerted during response inhibition. However, both factors can conjointly modulate inhibitory control. Cognitive theoretical concepts suggest that codings of stimulus-response translations may underlie such conjoint effects. Yet, it is unclear in how far such specific codes, as assumed in cognitive psychological concepts, are evident in neurophysiological processes and whether there are specific functional neuroanatomical structures associated with the processing of such codes. Applying a temporal decomposition method of EEG data in combination with source localization methods we show that there are different, intermingled codes (i.e., "stimulus codes" and "response selection codes") at the neurophysiological level during conjoint effects of "automatic" and "controlled" processes in response inhibition. Importantly, only "response selection codes" predict behavioral performance, and are subject to conjoint modulations by "automatic" and "controlled" processes. These modulations are associated with inferior and superior parietal areas (BA40/BA7), possibly reflecting an updating of internal representations when information is complex and probably difficult to categorize, but essential for behavioral control. Codes proposed by cognitive, psychological concepts seem to have a neurophysiological analogue that fits into current views on functions of inferior and superior parietal regions.

KEYWORDS
EEG, response inhibition, source localization

1 | INTRODUCTION

The inhibition of prepotent responses is a major requirement for goal-directed behavior and an important instance of cognitive control (Bari & Robbins, 2013). In the last years, a lot of research has been conducted to understand which factors determine successful response inhibition processes. Several lines of evidence suggest that one factor relates to the degree of automaticity of prepotent response tendencies (Chmielewski, Mückschel, Dippel, & Beste, 2015; Dippel, Chmielewski, Mückschel, & Beste, 2015; Donkers & van Boxtel, 2004; Helton, 2009; McVay & Kane, 2009; Mückschel, Chmielewski, Ziemssen, & Beste, 2017a), and that another factor relates to the degree of cognitive control that is exerted during response inhibition (Aron, 2007; Ridderinkhof, van den Wildenberg, Segalowitz, & Carter, 2004). While these factors may be regarded to be mutually exclusive, recent findings, however, suggest that both of these factors (i.e., "automaticity" and "cognitive control") exert conjoint effects (Chmielewski & Beste, 2016b) and that conflicts can foster response inhibition processes depending on how much response inhibition performance relies upon automatic or controlled processes.

To examine the interaction of automatic and controlled processes during response inhibition, these processes need to be dissociable at the experimental level. This can be achieved by combining a Go/NoGo with a Simon task in a "Simon Go/NoGo" task. In Simon tasks, conflicts occur depending on the congruency, or incongruence of stimulus laterality and response (motor) effector. No conflicts are evident in

congruent trials, because stimulus laterality and response effector are not different (stimulus on the left side of the monitor → left-handed utilization of the left response button; right-sided stimulus → right hand and response button). In incongruent trials a conflict occurs, because the stimulus laterality and the response effector are opposite to each other (left → right; right → left). These conflicts in the Simon task have been suggested to result from a combination of automatic and controlled processes (De Jong, Liang, & Lauber, 1994; Keye, Wilhelm, Oberauer, & Stürmer, 2013; Kornblum, Hasbroucq, & Osman, 1990; Mückschel, Stock, Dippel, Chmielewski, & Beste, 2016). One influential theoretical account to explain these conflict effects in Simon tasks is the dual-process account (De Jong et al., 1994). In this account, the automatic tendency to respond toward the stimulus location is labeled as "unconditionally automatic" process, or "direct route." The second process ("indirect route") involved is the conditional selection of the relevant stimulus feature(s) indicating the appropriate response. This is established by means of stimulus–response (S–R) bindings (specific stimulus → specific response effector) and requires the employment of cognitive control (Hommel, 2011). According to the dual-process account, in congruent trials "unconditionally automatic" processes alone can indicate the correct answer. Yet, in incongruent trials, a conflict between two mutually exclusive response tendencies ("unconditionally automatic" response tendencies indicating the stimulus laterality vs controlled conditional selection of stimulus features indicating the response button) emerges and complicates response selection processes (De Jong et al., 1994; Keye et al., 2013; Kornblum et al., 1990; Mückschel et al., 2016). When this dual-route logic was combined with a Go/NoGo task it has been shown that response inhibition is more difficult (error-prone), when processing is mediated via the unconditional-automatic route (congruent NoGo trials), compared to a condition where a conditional selection of the appropriate response is required (incongruent NoGo trials) (Chmielewski & Beste, 2016b). Even though this might be counterintuitive, the following has to be considered: For NoGo trials, it has been shown that response inhibition performance is more difficult when automated response tendencies are facilitated (Chmielewski et al., 2015; Dippel et al., 2015; Donkers & van Boxtel, 2004). This automaticity to execute a Go response in NoGo trials, should vary depending on the congruency of stimulus and response features (or automatic vs controlled processes). In incongruent NoGo trials, cognitive control is exerted to overcome "unconditionally automatic" processes *and* to resolve the conflict between the "unconditionally automatic" route and the appropriate conditional selection of stimulus features. This reduces the automaticity of inappropriate response tendencies in NoGo trials. Therefore, response inhibition performance is better under such conditions and conjoint effects of automated and controlled processes in NoGo trials can improve response inhibition performance (Chmielewski & Beste, 2016b). For congruent NoGo trials, however, less cognitive control is employed, because the "unconditionally automatic" route dominates processes. As a result, response inhibition is more difficult to exert and performance declines.

Importantly, the dual-process account also stresses the importance of stimulus (S)–response (R) translation processes as a major source driving effects in "Simon-like" paradigms (Hommel, 2011; Keye et al., 2013). Therefore, specific kinds of codes relating stimuli to responses are particularly important to consider for conjoint effects of controlled and automatic processes during response inhibition. Yet, the important and unresolved question is, in how far such specific codes during these processes can be isolated in neurophysiological processes and whether there are specific functional neuroanatomical structures associated with the processing of such codes? The question is whether a specific kind of code as suggested by cognitive, psychological concepts has a neurophysiological analog? If this would be the case, such a neurophysiological code should predict behavioral performance to a high degree.

Event-related potentials (ERP) may not be suitable to address such questions. This is because ERP components are composed of various amounts of signals from different sources (Huster, Plis, & Calhoun, 2015; Nunez et al., 1997; Stock, Gohil, Huster, & Beste, 2017). Moreover, and more relevant in the context of this study, ERPs can also reflect a mixture of different codes related to perceptual processing ("stimulus codes") and response selection ("response selection codes") (Folstein & Van Petten, 2008). In particular, "stimulus codes" and "response selection codes" can be intermingled at the neurophysiological level at any time point in the cognitive processing cascade. Regarding this, Mückschel et al. (2017a) have shown that there are not only consecutive levels of processing from stimulus selection (Boehler et al., 2009; Chmielewski & Beste, 2016a, 2016b) to response selection (Aron, Robbins, & Poldrack, 2014; Bari & Robbins, 2013). Rather, "stimulus codes" and "response selection codes" can co-exist over extended time periods during the inhibition of responses (Mückschel et al., 2017a). This is especially important to consider, when automatic ("unconditional") responding dominates behavior (Mückschel, Dippel, & Beste, 2017b). Similarly, it has long been argued that the N2 ERP component, a neurophysiological correlate of cognitive control and conflict monitoring (van Veen & Carter, 2002), reflects a concomitant coding of perceptual processes and of processes controlling for incorrect motor response preparation (Folstein & Van Petten, 2008). This is evident during the "conditional selection" of stimulus features (i.e., stimulus–response (S–R) binding) in the dual-route logic. The presence of dissociable fractions of "stimulus codes" and "response selection codes" in the N2 ERP component that are processed in overlapping areas of the medial frontal cortex, and that these are differentially modulated by neurobiochemical processes has recently been reported (Mückschel et al., 2017b).

To isolate "stimulus codes" and "response selection codes," an EEG temporal decomposition method, the residue iteration decomposition (RIDE) can be applied (Mückschel et al., 2017a; Ouyang, Herzmann, Zhou, & Sommer, 2011). Even though the primary purpose of RIDE is to account for intraindividual variability in EEG data (Ouyang et al., 2011; Ouyang, Sommer, & Zhou, 2015b), RIDE decomposes EEG data into several component clusters with dissociable functional relevance (Ouyang et al., 2011, 2015b). The S-cluster refers to stimulus-related processes (like perception and attention), the R-cluster refers to response-related processes (like motor preparation/execution), and the C-cluster refers to intermediate processes between S and R (like response selection) (Ouyang et al., 2011; Ouyang, Hildebrandt, Sommer, & Zhou, 2017). As response selection processes also take place for inappropriate responses in NoGo trials (Mostofsky &

Simmonds, 2008; Mückschel et al., 2017b), we will also utilize the term response selection processes for inhibitory trials in this paper.

In this study, we use RIDE to examine which of these codes are modulated by conjoint effects of "automaticity" and "cognitive control" during response inhibition. Combined with source localization methods, it is then possible to examine the associated functional neuroanatomical network (Mückschel et al., 2017a,b; Wolff, Mückschel, & Beste, 2017). The aforementioned stimulus (S)–response (R) translation processes have been suggested to be reflected by the C-cluster (Bluschke, Chmielewski, Mückschel, Roessner, & Beste, 2017; Mückschel et al., 2017a; Ouyang et al., 2017; Verleger, Metzner, Ouyang, Śmigasiewicz, & Zhou, 2014; Verleger, Siller, Ouyang, & Śmigasiewicz, 2017; Wolff et al., 2017), which has also been shown to be modulated during the inhibition of automated responses (Mückschel et al., 2017a) and is assumed to mostly reflect processes that are also assumed to be reflected by the (NoGo)-P3 (Mückschel et al., 2017b; Verleger et al., 2014, 2017; Wolff et al., 2017). During inhibitory control the C-cluster probably reflects a "braking function," or a mechanism that is important to inhibit automated response tendencies (Mückschel et al., 2017a). Therefore, we hypothesize that conjoint effects of "automaticity" and "cognitive control" during response inhibition are mostly reflected by modulations of "response selection codes" (the C-cluster) and not by modulations of "stimulus codes" (the S-cluster). This would suggest that specific kinds of code considered in cognitive, psychological concepts have a neurophysiological analogue. We hypothesize that these neurophysiological correlates reflect the interaction of "automaticity" and "cognitive control" processes during response inhibition and predict behavioral performance. More specifically, we expect more controlled (response selection) processes, as evident in incongruent (incongruent) inhibitory trials, to be reflected in an increased C-Cluster amplitude and in an improved response inhibition performance. For "unconditionally automated" processes, as evident congruent inhibitory trials, we expect the C-Cluster amplitude to be decreased. Because modulations in the C-cluster have been shown to be associated with functions of the medial frontal and/or inferior parietal regions (Mückschel et al., 2017a, 2017b; Ouyang et al., 2017; Wolff et al., 2017), we further hypothesize that these conjoint effects between "automaticity" and "cognitive control" processes are also correspondingly expressed within these areas. This is also likely because inferior parietal areas have been shown to be involved in response selection processes during the Simon task (Rushworth, Paus, & Sipila, 2001; Schiff, Bardi, Basso, & Mapelli, 2011).

2 | MATERIALS AND METHODS

2.1 | Sample

$N = 34$ young healthy participants (11 males) between 19 and 29 years (mean age 23.2 ± 0.7 years) took part in the experiment. All participants were free of medication, had normal or corrected-to-normal vision and hearing, and reported no neurological or psychiatric disorders. Written informed consent was obtained from all participants. This study was approved by the institutional review board of the Medical faculty of the TU Dresden.

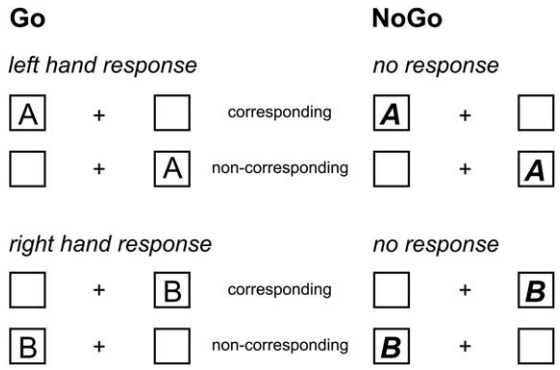

FIGURE 1 Schematical illustration of the experimental paradigm showing all experimental conditions. In the left panel, "GO" trials are shown, whereas in the right panel, "NoGo" trials are shown. The upper row shows the condition requiring left hand responses on Go trials (responses on stimulus "A"), the lower row right hand responses on Go trials (responses on stimulus "B")

2.2 | Task

To examine the relevance of concomitantly processed "stimulus codes" and "response selection codes" for conjoint effects of "automaticity" and "cognitive control" during response inhibition, we use a combined Simon-Go/NoGo task. The outline of the task is shown in Figure 1.

White stimuli were presented on a black background (57cm viewing distance). A fixation cross was continuously presented in the middle of screen and one white boxes at the same vertical level were presented on the left and right of the fixation cross (distance of 1.1° visual angle). Each trial began with the presentation of a letter (for 200 ms) in one of the white frame boxes and subjects were required to press within 1200 ms (on Go trials). On each trial a letter stimulus in normal font (i.e., "A," "B"), or in bold-italics (i.e., "***A***" or "***B***") was presented. Participants were requested to respond as fast as possible to letters in a normal font (i.e., A and B; Go trials), while responses had to be inhibited, whenever the letter stimuli were presented in the combined bold and italic font (i.e., "***A***" and "***B***"; NoGo trials). For Go trials, whenever an "A" was displayed, a left-hand response was required, whereas a right-hand response was required, whenever a "B" was displayed. These responses were required regardless of the spatial position of the letter stimuli in the left or right white frame box on the screen. This constituted two different Go conditions, that is, a congruent Go condition where stimuli were presented on the side of the hand carrying out the response and one incongruent condition where stimuli were presented on the side opposite of the hand carrying out the response. For NoGo trials (combined bold and italic font letters), left-side "***A***"s and right-side "***B***"s represented congruent NoGo trials, whereas left-side "***B***"s and right-side "***A***"s represented incongruent NoGo trials. This variation of congruency in Go and NoGo trials created the Simon component in the task. The task conditions are shown in Figure 1.

If no response was given on Go trials in a time window of 500 ms, a speed-up sign ("Schneller!") was presented above the fixation cross. Each trial ended after 1700 ms, if no response was previously recorded. The intertrial interval (ITI) was jittered between 1100 and 1600 ms. The experiment consisted of 720 trials [70% (504 trials) Go and 30%

(216 trials) NoGo trials], of which 50% were congruent and 50% were incongruent. The experiment was divided into six blocks with 120 trials each. Trial types (congruent and incongruent Gos, or congruent and incongruent NoGos) were presented randomly, but it was ensured that all conditions were equally distributed across the blocks. Before the experiment, each subject was trained on the task using 40 trials.

During Go trials, a response had to be executed within the time interval from 250 to 1200 ms. An incorrect response in that time-window was coded as error and if no response was obtained, trials were coded as misses. For NoGo trials, any response resulted in trials being coded as false alarms. These behavioral parameters were acquired for congruent and incongruent trials separately.

2.3 | EEG recording and analysis

The EEG was recorded using 60 Ag/AgCl electrodes (sampling rate 500 Hz) connected to a "BrainAmp" amplifier (Brain Products Inc.). The electrode impedances were kept below 5 kΩ. The reference electrode was located at Fpz and the ground electrode was located at $\theta = 58$, $\phi = 78$. Offline, a band-pass filter from 0.5 to 20 Hz (48 dB/oct slope each) was applied and the EEG was downsampled to 256 Hz. Then, a raw data inspection was conducted to remove technical artifacts, while periodically occurring artifacts such as pulse artifacts, horizontal, and vertical eye movements were subsequently detected and corrected for by means of an independent component analysis (ICA; infomax algorithm). After these corrections, cue-locked segments were formed according to the experimental conditions: congruent Go trials, incongruent Go trials, congruent NoGo trials, and incongruent NoGo trials. Only trials with correct responses were included. The segments started 200 ms prior to the locking point (cue onset was set to time point 0) and ended 1200 ms thereafter. Afterward, an automated artifact rejection procedure was applied using a maximal value difference above 200 μV in a 200 ms interval and an activity below 0.5 μV in a 100 ms period as rejection criteria. Overall, ~1.2% of trials were discarded on the basis of these criteria and there was no difference between conditions [$t(33) = -0.49$, $p > .6$]. Then, a current source density (CSD) transformation was run, which eliminates the reference potential from the data and helps to find the electrodes showing the strongest effects (Nunez & Pilgreen, 1991). The resulting CSD values are stated in $\mu V/m^2$. A baseline correction was then set to a time interval from −200 to 0 ms (i.e., stimulus presentation) before the segments were averaged. The ERP components were quantified on the single-subject level using the mean amplitude in a specific time interval. Time windows and electrode sites were chosen on the basis of a literature-driven visual inspection of the ERPs and corresponding topography maps in highly probable time windows. This choice of electrodes and time windows was validated using following statistical method (Mückschel, Stock, & Beste, 2014): within each of the visually detected search intervals (see below), the peak amplitude was extracted for all 60 electrodes. Each electrode was subsequently compared against the average of all other electrodes using Bonferroni-correction for multiple comparisons (critical threshold $p = .0007$). Only electrodes that showed significantly larger mean amplitudes (i.e., negative for N-potentials and positive for the P-potentials) than the remaining electrodes were selected. This pattern of electrodes matched the electrodes found in the visual inspection of the data. Consequently, the P1 ERP component was quantified at electrodes P7 and P8 in the time interval from 95 to 110 ms; the N1 ERP-component was quantified at electrodes P7 and P8 in the time interval from 155 to 170 ms in Go and NoGo trials. The N2 and P3 ERP-components were quantified in a time window of 310–340, or respectively 480–520 ms at electrodes FCz and Cz in Go and NoGo trials.

2.4 | Residue iteration decomposition (RIDE)

To dissociate "stimulus codes" from "response selection codes," residue iteration decomposition (RIDE) was run using established protocols (Mückschel et al., 2017a; Ouyang et al., 2011; Verleger et al., 2014) and the RIDE toolbox and manual (available on http://cns.hkbu.edu.hk/RIDE.htm). RIDE decomposes ERP components applying *L1*-norm minimization (i.e., obtaining median waveforms) and therefore minimizes residual error due to noise in the data (Ouyang, Sommer, & Zhou, 2015a; Ouyang et al., 2015b). Importantly, these spatial filter properties of the CSD do not violate assumptions relevant to RIDE since the decomposition is conducted separately for each single electrode channel (Ouyang et al., 2015b).

RIDE decomposes the ERP signal into clusters that are either correlated to the stimulus onset (S-cluster or to the response time (R-cluster), and a central C-cluster with variable latency, which is estimated initially and iteratively improved. Since no response time measure can be collected in NoGo trials when no button press is required, it is not possible to depict processes related to the response (Ouyang, Schacht, Zhou, & Sommer, 2013). Therefore, the R-cluster was not computed. RIDE uses a self-optimized iteration scheme for latency estimation through which the latency estimation of the C-cluster is improved. In the RIDE algorithm, the initial latency of the C-cluster is estimated using a time window function. In an iterative procedure, the S-cluster is removed, and the latency of the C-cluster is re-estimated based on a template matching approach until convergence of the initial latency estimation and the S- and C-cluster. Full mathematical details of the RIDE method, including information about the validity of the template matching approach used by the RIDE algorithm can be found in methodological papers on the RIDE procedure (Ouyang et al., 2011, 2013, 2015b). The validity of the RIDE procedure for Go/Nogo tasks has already been shown (Mückschel, Dippel, & Beste, 2017c; Ouyang et al., 2013). During processing, the initial time window for the estimation of the C-cluster was set to 200–700 ms after stimulus onset. The time window is assumed to cover the range within which each component is supposed to occur (Ouyang et al., 2015a). The time window for the S-cluster was set to −200 to 400 ms around stimulus onset. For further details on the method, see Ouyang et al. (2011, 2015a) and for a detailed analysis of NoGo tasks using RIDE, please refer to Ouyang et al., (2013). The procedure used here is exactly the same as done in Ouyang et al. (2013) and Mückschel et al. (2017a).

For data quantification, a visual inspection of the data was performed, which was also followed by the statistical validation

procedures described for the ERP-component data. The S-cluster was quantified at electrodes P7 and P8 as well as electrode FCz in Go and NoGo trials. At electrodes P7 and P8, the mean amplitude in the P1 time window was quantified in the time interval from 95 to 110ms, and in the N1 time window in the time interval from 155 to 170ms in Go and NoGo trials. At electrode FCz, data was quantified in the N2 time window between 310 and 340ms. For the C-cluster, it has already been shown that it reflects processes that are commonly reflected by the (NoGo)-P3 ERP component (Ouyang et al., 2017; Verleger et al., 2014; Wolff et al., 2017). The C-cluster was quantified in Go and NoGo trials. The C-cluster revealed negative amplitudes at central electrodes (i.e., Cz) between 310 and 340 ms and positive amplitudes at centro-parietal electrode sites (i.e., CPz, Pz, and P1) between 440 and 490 ms. C-cluster amplitudes were quantified at these electrodes and time windows. The statistical validation procedure confirmed this choice of electrodes and time windows.

2.5 | Source localization

The source localization was conducted using the RIDE data, as we were especially interested in the sources associated with the processing of dissociable "stimulus codes" and "response selection codes." The analysis was performed using sLORETA (standardized low resolution brain electromagnetic tomography; Pascual-Marqui, 2002). sLORETA provides a single linear solution to the inverse problem without a localization bias (Marco-Pallarés, Grau, & Ruffini, 2005; Pascual-Marqui, 2002; Sekihara, Sahani, & Nagarajan, 2005). There is also evidence of EEG/fMRI and EEG/TMS studies underlining the validity of the sources estimated using sLORETA (Dippel & Beste, 2015; Sekihara et al., 2005). For sLORETA, the intracerebral volume is partitioned into 6239 voxels at 5 mm spatial resolution. The standardized current density at each voxel is calculated in a realistic head model using the MNI152 template. As this study focuses on the modulation of RIDE clusters during response inhibition processes by the congruent and incongruent conditions, the voxel-based sLORETA images compared NoGo trials in the congruent Simon condition against NoGo trials in the incongruent Simon condition. Comparisons were based on statistical nonparametric mapping (SnPM) using the sLORETA-built-in voxel-wise randomization tests with 2000 permutations. Voxels with significant differences ($p < .01$, corrected for multiple comparisons) between contrasted conditions were located in the MNI brain www.unizh.ch/keyinst/NewLORETA/sLORETA/sLORETA.htm

2.6 | Statistics

The behavioral data were analyzed using dependent samples *t* tests. The neurophysiological data (i.e., ERPs and RIDE clusters) were analyzed using repeated measures ANOVAs including the factor "condition" (Go vs NoGo) and "congruency" (congruent vs incongruent) as within-subject factors. Greenhouse–Geisser correction was applied where appropriate. All post-hoc tests were Bonferroni-corrected. All variables included in the analyses were normal distributed as indicated by Kolmogorov–Smirnov Tests (all $z < 0.85$; $p > .3$).

3 | RESULTS

3.1 | Behavioral data

For the behavioral data, a dependent samples *t* test showed that reaction times (RTs) were longer on incongruent (545 ms ± 14) than congruent Go trials (517 ms ± 13) ($t(33) = -7.83$; $p < .001$). The hit rate on Go trials was larger on congruent trials (94.8% ± 0.65) than on incongruent trials (91.3% ± 1.2) ($t(33) = 3.31$; $p = .001$). However, the rate of false alarms (responses executed in NoGo trials) is the most important behavioral parameter in response inhibition paradigms. The rate of false alarms was larger in congruent NoGo trials (14.62% ± 1.95) than in incongruent NoGo trials (9.58% ± 1.25) ($t(33) = 4.04$; $p < .001$).

3.2 | Neurophysiological data

3.2.1 | Event-related potentials (ERPs)

The standard event-related potentials are shown in Figure 2.

For the N2 ERP component (Figure 2a), analysis revealed a main effect "congruency" ($F(1,33) = 6.97$; $p = .013$; $\eta_p^2 = .174$) showing that the N2 was larger (i.e., more negative) on incongruent (−11.05 μV/m² ± 1.52) than on congruent trials (−8.15 μV/m² ± 1.99). The main effect "Go/NoGo" ($F(1,33) = 26.76$; $p < .001$; $\eta_p^2 = .448$) revealed that the N2 was more negative in NoGo (−12.87 μV/m² ± 1.57) than in Go trials (−6.33 μV/m² ± 2.01) and the sLORETA analysis suggests that this relates to activation differences in the right inferior frontal gyrus. This area has frequently been reported to reflect inhibitory control processes (Aron et al., 2014). There was an interaction "congruency × Go/NoGo" ($F(1,33) = 6.98$; $p = .013$; $\eta_p^2 = .174$). Post-hoc tests revealed that the difference in N2 amplitudes between Go and NoGo trials (i.e., the response inhibition effect) was larger in the incongruent condition (−7.43 μV/m² ± 1.45) than in the congruent condition (−3.63 μV/m² ± 1.30) ($t(33) = 2.64$; $p = .013$).

For the P3 ERP component (Figure 2a), the was only a main effect "Go/NoGo" ($F(1,33) = 63.63$; $p < .001$; ηp2 = .659), showing that the P3 was larger in NoGo (11.72 μV/m² ± 2.5) than in Go trials (−3.77 μV/m² ± 2.5). No other main or interaction effects were significant (all $F < 1.47$; $p > .2$).

For the P1 ERP component, and for the N1 ERP component (Figure 2b), the repeated measures ANOVA revealed no main or interaction effects (all $F < 1.1$; $p > .3$)

3.3 | RIDE-decomposition

3.3.1 | S-cluster

The S-cluster, including scalp topography plots is shown in Figure 3.

As expected, the S-cluster was evident at fronto-central electrode sites in the N2 ERP-component time window (Figure 3a), which is in line with previous results (Mückschel et al., 2017a) and in line with concepts stating that the N2 reflects a mixture of stimulus and response-related processes (Folstein & Van Petten, 2008). Moreover, the S-cluster reflected activity in the time range of the P1 and N1 ERP-components (Figure 3b). Interestingly, for all time windows and

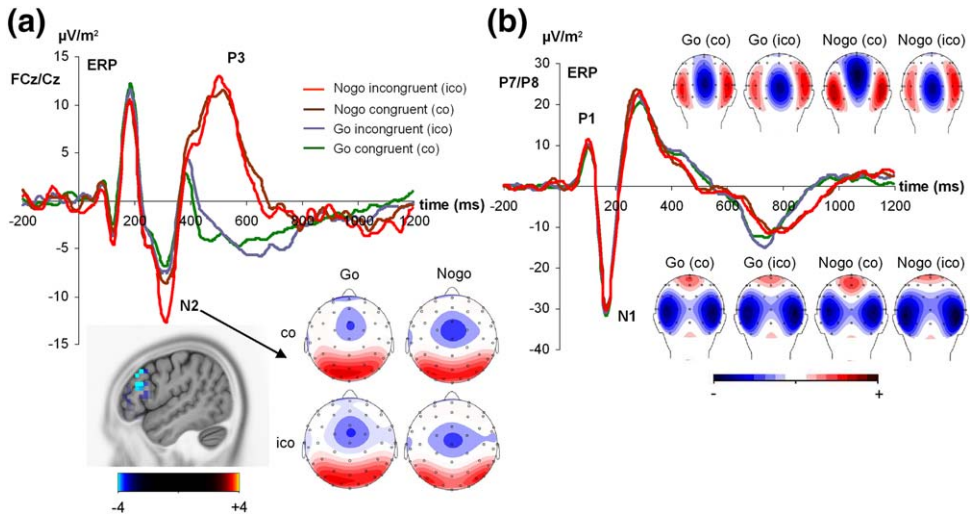

FIGURE 2 (a) Event-related potentials (ERPs) showing the N2 and P3 ERP-component at electrodes FCz/Cz in all four experimental conditions including the scalp topography plots. The sLORETA plot shows the comparison between Go and NoGo trials in the N2 time window. The source shown is corrected for multiple comparison using SnPM ($p < .01$). The color scale denotes critical t values. A source in the right inferior frontal gyrus is shown. (b) The P1 and N1 ERP-components (at electrodes P7/P8) are shown for all conditions including the scalp topography plots. The scalp topography plots show the distribution of potentials at the peak of each ERP component. In the scalp topography plots, blue colors denote negativity and red colors denote positivity [Color figure can be viewed at wileyonlinelibrary.com]

electrodes analyzed in the S-cluster, there were no main or interaction effects (all $F < 0.24$; $p > .85$). For the S-cluster, it is not possible to compare Go and NoGo trials using sLORETA because there were no amplitude differences. We, however, compared the N2 in NoGo trials against zero. This contrast also revealed a source in the right inferior frontal gyrus (refer to Figure 3). There are thus converging sources for the S-cluster in the N2 time window in NoGo trials and the NoGo-N2 at the ERP level. This further validates the sLORETA results based on RIDE data.

As this lack of effects in the S-cluster in the N2 time window is important from a theoretical point of view (refer introduction) we calculated bayesian statistics. Opposed to classical null hypothesis testing using ANOVAs, Bayesian statistics (Masson, 2011; Wagenmakers, 2007) can evaluate the relative strength of evidence for the null hypothesis (Masson, 2011). It is possible to examine the probability of the null hypothesis being true, given the obtained data ($p(H_O|D)$) and can be achieved on the basis of a transformation of the sum-of-squares values generated by the ANOVA (Masson, 2011). This analysis revealed

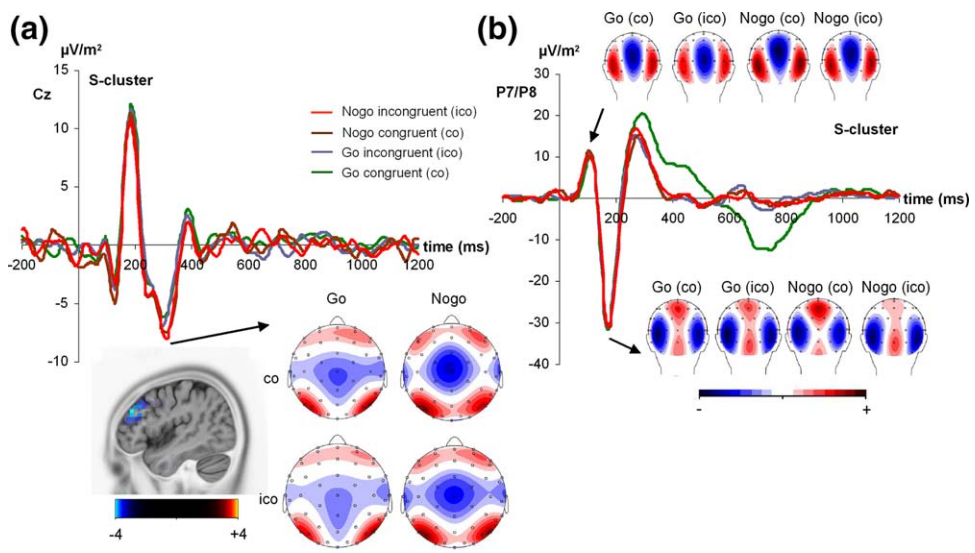

FIGURE 3 This figure shows the S-cluster data at electrode Cz for the N2 time window (a) and for the P1 and N1 time window. The sLORETA plot shows the comparison NoGo trials against zero (NoGo < 0) in the N2 time window. The source shown is corrected for multiple comparison using SnPM ($p < .01$). The color scale denotes critical t values. A source in the right inferior frontal gyrus is shown. (b). All experimental conditions are shown. The scalp topographies show the distribution of potentials at the peak of the S-cluster in the N2 and P1/N1 time window. In the scalp topography plots, blue colors denote negativity and red colors denote positivity [Color figure can be viewed at wileyonlinelibrary.com]

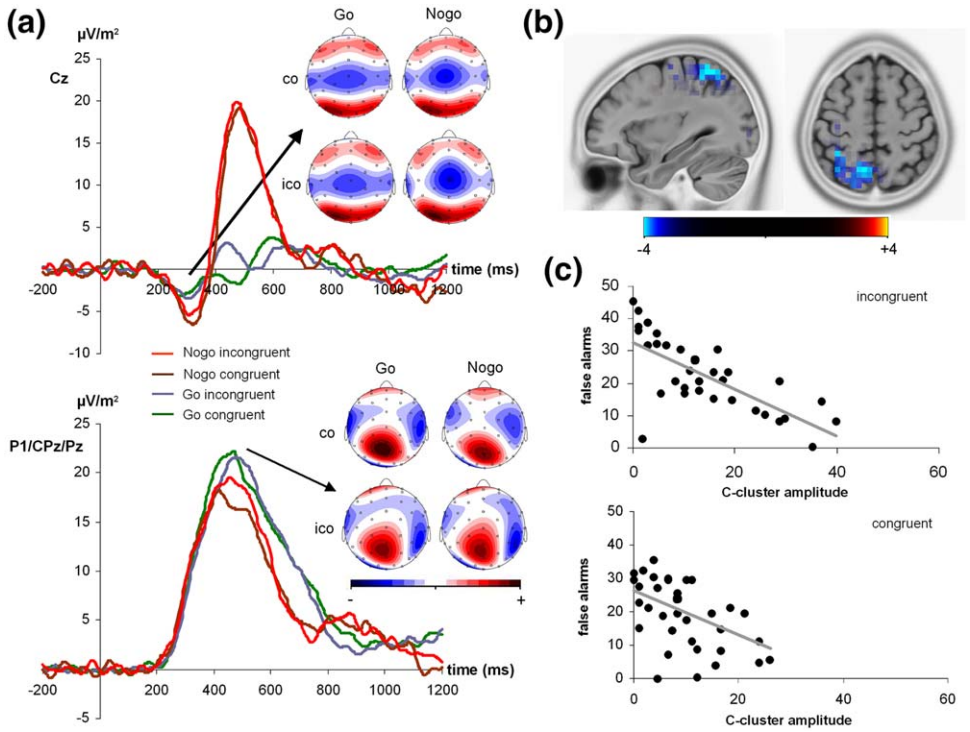

FIGURE 4 (a) The C-cluster is shown at electrodes Cz and P1/CPz/Pz for all experimental conditions, including the scalp topographies. The scalp topographies show the distribution of potentials at the peak of the C-cluster at the shown electrodes. In the scalp topography plots, blue colors denote negativity and red colors denote positivity. (b) Results from the sLORETA analysis comparing the congruent and incongruent NoGo trials. The source shown is corrected for multiple comparison using SnPM ($p < .01$). The color scale denotes critical t values. (c) Scatterplots showing the negative correlation between the C-cluster amplitude and the false alarms in the incongruent (top) and the congruent condition (bottom) [Color figure can be viewed at wileyonlinelibrary.com]

$p(H_0|D) > .95$. The results of the Bayesian analysis show that there is strong evidence in favor for the null hypothesis that no modulations are evident in the S-cluster.

3.3.2 | C-cluster

The C-cluster, including scalp topography plots is shown in Figure 4a. As can be seen in Figure 4, The C-cluster revealed negative amplitudes at central electrodes (i.e., Cz) and positive amplitudes at centro-parietal electrode sites (i.e., CPz, Pz, and P1).

For the central negativity, the repeated measures ANOVA only revealed a main effect "Go/NoGo" ($F(1,33) = 6.95$; $p = .013$; $\eta_p^2 = .174$), showing that the C-cluster was more negative on NoGo trials ($-4.32\ \mu V/m^2 \pm 1.47$) than on Go trials ($-2.21\ \mu V/m^2 \pm 1.45$). All other main or interaction effects were not significant (all $F < 0.66$; $p > 4.$). Since the Bayesian analysis revealed $p(H_0|D) > .90$, there is strong evidence in favor for the null hypothesis.

For the parietal positivity, the repeated measures ANOVA revealed a main effect "congruency" ($F(1,33) = 6.61$; $p = .015$; $\eta_p^2 = .167$) showing that the C-cluster was larger in the incongruent ($23.89\ \mu V/m^2 \pm 1.83$) than in the congruent condition ($20.42\ \mu V/m^2 \pm 1.84$). The main effect "electrode" ($F(2,66) = 7.75$; $p = .001$; $\eta_p^2 = .190$) revealed that the C-cluster was largest at electrode Pz ($26.22\ \mu V/m^2 \pm 2.53$) and differed from electrode CPz ($18.38\ \mu V/m^2 \pm 1.78$) and electrode P1 ($21.86\ \mu V/m^2 \pm 1.77$) ($p = .008$). Electrodes CPz and P1 did not differ from each other ($p > .3$). The main effect Go/NoGo ($F(1,33) = 5.61$; $p = .024$; $\eta_p^2 = .145$) showed that the C-cluster was larger on Go ($22.85\ \mu V/m^2 \pm 1.80$) than on NoGo trials ($21.46\ \mu V/m^2 \pm 1.65$). Importantly, there was an interaction "congruency × Go/NoGo" ($F(1,33) = 10.10$; $p = .003$; $\eta_p^2 = .234$). Post-hoc dependent samples t tests revealed that there was no difference in the C-cluster amplitude on Go trials ($t(33) = -0.80$; $p > .4$), while there was a difference on NoGo trials ($t(33) = 3.35$; $p = .001$) showing that the C-cluster was larger on incongruent ($22.08\ \mu V/m^2 \pm 1.96$) than on congruent trials ($18.76\ \mu V/m^2 \pm 1.83$). No other main or interaction effects were significant (all $F < 0.49$; $p > .6$). Using sLORETA the congruent and incongruent NoGo trials were contrasted to examined the associated source. This analysis shows that modulations in the C-cluster amplitude ($NoGo_{congruent} < NoGo_{incongruent}$) were associated with activation differences in the left superior parietal cortex (BA7) and the left inferior parietal cortex (BA40) including the temporo-parietal junction (refer Figure 4b). For a discussion on the different congruency effects for NoGo trials at posterior and fronto-central electrode sites, as well as a discussion on the larger C-cluster amplitudes in Go than NoGo trials, the reader is kindly referred to the Supporting Information.

3.4 | Correlation analyses

To examine whether the C-cluster systemically predicts performance Pearson correlations were conducted. The scatterplots are shown in Figure 4c. For the incongruent NoGo trials, the C-cluster amplitude in

the P3 time window at parietal electrodes was negatively correlated with the rate of false alarms in that condition ($r = -.608$; $R^2 = 36.9$; $p < .001$); that is, the higher the C-cluster's amplitude, the lower the rate of false alarms. A similar correlation was observed for the congruent condition ($r = -.585$; $R^2 = 34.2$; $p < .001$). For the C-cluster amplitudes in the N2 time window, no correlations were obtained (all $r < -.114$; $p > .2$) and the same was the case for the C-cluster amplitude in Go trials (all $r < -.054$; $p > .4$). No correlations were obtained for the S-cluster data for Go and NoGo trials (all $r < -.132$; $p > .2$) and also in ERP-component's amplitudes in all examined time windows for Go and NoGo trials (all $r < -.095$; $p > .3$). Together, only the C-cluster amplitudes in NoGo trials, but no other neurophysiological parameter predicted behavioral performance.

4 | DISCUSSION

Goal of this study was to examine whether conjoint effects of "automaticity" and "cognitive control" during response inhibition are reflected by specific neurophysiological codes and whether specific functional neuroanatomical structures are involved in this coding. These questions relate to theoretical considerations and previous evidence suggesting that different, intermingled codes ("stimulus codes" and "response selection codes") at the neurophysiological level may be crucial for conjoint effects of "automaticity" and "cognitive control" during response inhibition. To examine this question, we applied residue iteration decomposition (RIDE) to ERP data and combined this with source localization methods (sLORETA).

The behavioral data were well in line with literature on the Simon task: RTs and error rates were increased in conflicting (i.e., incongruent), compared to nonconflicting (congruent) stimulus–response (S–R) relations (Keye et al., 2013). More important, and in accordance with a previous study, it was shown that congruent stimulus–response relations during inhibitory trials lead to an increase in false alarms (Chmielewski & Beste, 2016b). The finding that conflicts can foster response inhibition performance, while they aggravate response execution processes can be explained using the dual-process account (De Jong et al., 1994): According to this account, the first process reflects stimulus evoked automatic tendency to respond towards the stimulus location via the "direct route." The second process reflects a conditional (controlled) selection of the relevant feature(s) and the response via the "indirect route." When applying this logic to NoGo trials, a conflict occurs between the "direct" and "indirect route" whenever there is an incongruent stimulus–response relation. This results in an increased deployment of cognitive control. This increased deployment of cognitive control decreases the automaticity of response execution (i.e., to react in NoGo trials) and fosters response inhibition performance. In congruent NoGo conditions, this additional deployment of cognitive control is not initiated and response inhibition performance becomes worse. Therefore, conjoint effects of "automaticity" and "cognitive control" can modulate (or improve) response inhibition performance (Chmielewski & Beste, 2016b).

These behavioral results were paralleled by specific effects in the neurophysiological data. In the N2 amplitude, an interaction "Go/NoGo x congruency" was observed. Amplitude differences between Go and NoGo trials were larger for the incongruent condition than the congruent condition. As the N2 amplitude is assumed to reflect conflict monitoring and premotor inhibition processes (Chmielewski & Beste, 2015; Donkers & van Boxtel, 2004; Falkenstein, Hoormann, & Hohnsbein, 1999; Nieuwenhuis, Yeung, & Cohen, 2004), increased amplitudes in NoGo and/or incongruent trials are well in line with the literature. However, the N2 reflects a concomitant coding of perceptual processes and motor processes (Folstein & Van Petten, 2008; Mückschel et al., 2017b). When applying RIDE to dissociate between these different codes, it was shown that conjoint effects of "automaticity" and "cognitive control" during response inhibition, only affected the response selection codes, but not stimulus codes.

No conjoint effects of "automaticity" and "cognitive control" were evident in the S-cluster because no interaction effect "congruency × Go/NoGo" was evident. This was substantiated by a Bayesian analysis of the data and is in line with the study hypothesis. Only for the C-cluster (response selection codes) data, an interaction "Go/NoGo × congruency" was observed at parietal electrode sites. This interaction is due to nonsignificant differences in C-cluster amplitudes between congruent and incongruent Go trials, but increased C-cluster amplitudes in incongruent, compared to congruent NoGo trials. Besides reflecting "response selection codes"-related processes mediating between stimulus evaluation and responding (Bluschke et al., 2017; Mückschel et al., 2017a; Ouyang et al., 2017; Verleger et al., 2014, 2017; Wolff et al., 2017), the C-cluster has also been assumed to reflect a "braking function" for motor processes (Mückschel et al., 2017b). The decreased C-cluster amplitude in congruent NoGo trials compared to incongruent NoGo trials likely reflects an insufficient braking of motor responses. This may be an effect of stronger "automatic" processes in congruent NoGo trials. The finding that the C-cluster and response selection codes underlie conjoint effects of controlled and automatic processes during response inhibition is further substantiated by the findings of the regression analyses. Increased C-cluster amplitudes in inhibitory trials were related to better inhibitory control performance (lower false alarms) in congruent and incongruent trials. As no such correlations were obtained for the S-cluster or the ERP data, this shows that especially "response selection codes" are essential for conjoint effects of "automaticity" and "cognitive control" during response inhibition.

The finding that especially "response selection codes" (i.e., the C-cluster) are modulated during NoGo trials is consistent with cognitive theoretical accounts of the experimental rationale of this study: According to the dual-process account (De Jong et al., 1994), stimuli evoke an automatic response tendency to respond toward their location ("automatic process") via the "direct route." The second process, via the "indirect route," reflects a conditional selection of the relevant feature(s) and the appropriate response. The dual-process account stresses the importance of stimulus (S)–response (R) translation processes as a major source driving effects in "Simon-like" paradigms (Hommel, 2011; Keye et al., 2013). Exactly such S–R translations processes have been suggested to be reflected by the C-cluster (Bluschke et al.,

2017; Mückschel et al., 2017a; Ouyang et al., 2017; Verleger et al., 2014, 2017; Wolff et al., 2017). Also horse race models stress the importance of S–R translation processes (Band, Ridderinkhof, & van der Molen, 2003b). The horse race framework assumes that Go and NoGo processes race for execution and that the more dominant process gets executed (Band, van der Molen, & Logan, 2003a; Logan, Cowan, & Davis, 1984; Logan, Van Zandt, Verbruggen, & Wagenmakers, 2014). In this framework, conflicting stimulus response translations impede Go processes and hence increase the probability that NoGo processes are executed. In congruent, nonconflicting stimulus response relations Go processes are not impeded, which results in a quicker response execution and consequently in increased false alarm rates. Together, the dual-process account and horse race models are in line with the finding that especially the modulation of response selection codes (reflected by the C-cluster) underlies conjoint effects of controlled and automatic processes during response inhibition.

The source localization, contrasting the congruent and incongruent NoGo conditions, revealed that regions in the left inferior parietal cortex (BA40) encompassing the temporo-parietal junction (TPJ) and the left superior parietal lobe (BA7) were associated with modulations in "response selection codes" in the C-cluster amplitude. Neural activity in these areas was increased in the incongruent compared to the congruent NoGo condition. Especially the involvement of the TPJ (BA40) seems plausible, as this region has been shown to be involved in response selection processes during the Simon task. Here, the TPJ is assumed transform spatial information into code for action (Rushworth et al., 2001; Schiff et al., 2011). In line with that, also more recent concepts suggest that the TPJ processes task-relevant stimuli to update internal representations of the environmental context using sensory information to initiate appropriate actions (Geng & Vossel, 2013). This concept closely resembles "response selection codes" likely reflected by the C-cluster. Yet, also the involvement of superior parietal regions (BA7) closely relates to these aspects. Even though the superior parietal cortex (BA7) has less frequently been reported to be involved in response inhibition (Barber, Caffo, Pekar, & Mostofsky, 2013; Dippel et al., 2015; Fan, Gau, & Chou, 2014; Ocklenburg, Güntürkün, & Beste, 2011), it has been suggested that the BA7 is involved in response inhibition, whenever it is essential, but challenging, to categorize complex information to inform inhibitory processes (Fokin et al., 2008; Ocklenburg et al., 2011; Takeichi et al., 2010). From this perspective, it seems reasonable that activity in BA7 was increased in the incongruent NoGo condition, because in this condition the selection of (inappropriate Go) responses is complicated by the conflict between the automatic response tendency to respond towards their location ("automatic process") mediated via the "direct route" and the conditional (controlled) selection of the relevant feature(s), mediated via the "indirect route."

In summary, this study shows that there are different, intermingled codes (i.e., "stimulus codes" and "response selection codes") at the neurophysiological level during conjoint effects of "automaticity" and "cognitive control" on response inhibition. Especially "response selection codes" predict behavioral performance, and are subject to modulations by "automatic" and "controlled" processes. This study shows that codes considered to be important from a cognitive psychological point of view can be isolated in neurophysiological processes using temporal EEG signal decomposition. Moreover, these codes can be related to specific functional neuroanatomical structures using source localization. In this study, parietal areas are modulated, which is again well in line with current concepts about the functional relevance of inferior and superior parietal regions.

ACKNOWLEDGMENT

This work was supported by a grant from the Deutsche Forschungsgemeinschaft (DFG) SFB 940 project B8.

ORCID

Witold X. Chmielewski http://orcid.org/0000-0003-4410-3709
Christian Beste http://orcid.org/0000-0002-2989-9561
Moritz Mückschel http://orcid.org/0000-0002-9069-7803

REFERENCES

Aron, A. R. (2007). The neural basis of inhibition in cognitive control. *The Neuroscientist: A Review Journal Bringing Neurobiology, Neurology and Psychiatry*, *13*, 214–228.

Aron, A. R., Robbins, T. W., & Poldrack, R. A. (2014). Inhibition and the right inferior frontal cortex: One decade on. *Trends in Cognitive Sciences*, *18*, 177–185.

Band, G. P. H., van der Molen, M. W., & Logan, G. D. (2003a). Horse-race model simulations of the stop-signal procedure. *Acta Psychologica*, *112*, 105–142.

Band, G. P. H., Ridderinkhof, K. R., & van der Molen, M. W. (2003b). Speed-accuracy modulation in case of conflict: The roles of activation and inhibition. *Psychological Research*, *67*, 266–279.

Barber, A. D., Caffo, B. S., Pekar, J. J., & Mostofsky, S. H. (2013). Developmental changes in within- and between-network connectivity between late childhood and adulthood. *Neuropsychologia*, *51*, 156–167.

Bari, A., & Robbins, T. W. (2013). Inhibition and impulsivity: Behavioral and neural basis of response control. *Progress in Neurobiology*, *108*, 44–79.

Bluschke, A., Chmielewski, W. X., Mückschel, M., Roessner, V., & Beste, C. (2017). Neuronal intra-individual variability masks response selection differences between ADHD subtypes-A need to change perspectives. *Frontiers in Human Neuroscience*, *11*, 329.

Boehler, C. N., Münte, T. F., Krebs, R. M., Heinze, H.-J., Schoenfeld, M. A., & Hopf, J.-M. (2009). Sensory MEG responses predict successful and failed inhibition in a stop-signal task. *Cerebral Cortex (New York, N.Y.: 1991)*, *19*, 134–145.

Chmielewski, W. X., & Beste, C. (2015). Action control processes in autism spectrum disorder – Insights from a neurobiological and neuroanatomical perspective. *Progress in Neurobiology*, *124*, 49–83.

Chmielewski, W. X., & Beste, C. (2016a). Perceptual conflict during sensorimotor integration processes - a neurophysiological study in response inhibition. *Scientific Reports*, *6*, 26289.

Chmielewski, W. X., & Beste, C. (2016b). Testing interactive effects of automatic and conflict control processes during response inhibition - A system neurophysiological study. *NeuroImage*,

Chmielewski, W. X., Mückschel, M., Dippel, G., & Beste, C. (2015). Concurrent information affects response inhibition processes via the modulation of theta oscillations in cognitive control networks. *Brain Structure and Function*, 1–13.

De Jong, R., Liang, C. C., & Lauber, E. (1994). Conditional and unconditional automaticity: A dual-process model of effects of spatial stimulus-response correspondence. *Journal of Experimental Psychology. Human Perception and Performance*, *20*, 731–750.

Dippel, G., & Beste, C. (2015). A causal role of the right inferior frontal cortex in the strategies of multi-component behaviour. *Nature Communications*.

Dippel, G., Chmielewski, W., Mückschel, M., & Beste, C. (2015). Response mode-dependent differences in neurofunctional networks during response inhibition: An EEG-beamforming study. *Brain Structure and Function*.

Donkers, F. C. L., & van Boxtel, G. J. M. (2004). The N2 in go/no-go tasks reflects conflict monitoring not response inhibition. *Brain and Cognition*, *56*, Neurocognitive mechanisms of performance monitoring and inhibitory control:165–176.

Falkenstein, M., Hoormann, J., & Hohnsbein, J. (1999). ERP components in Go/Nogo tasks and their relation to inhibition. *Acta Psychologica*, *101*, 267–291.

Fan, L.-Y., Gau, S. S.-F., & Chou, T.-L. (2014). Neural correlates of inhibitory control and visual processing in youths with attention deficit hyperactivity disorder: A counting Stroop functional MRI study. *Psychological Medicine*, *44*, 2661–2671.

Fokin, V. A., Shelepin, Y. E., Kharauzov, A. K., Trufanov, G. E., Sevost'yanov, A. V., Pronin, S. V., & Koskin, S. A. (2008). Localization of human cortical areas activated on perception of ordered and chaotic images. *Neuroscience and Behavioral Physiology*, *38*, 677–685.

Folstein, J. R., & Van Petten, C. (2008). Influence of cognitive control and mismatch on the N2 component of the ERP: A review. *Psychophysiology*, *45*, 152–170.

Geng, J. J., & Vossel, S. (2013). Re-evaluating the role of TPJ in attentional control: Contextual updating? *Neuroscience and Biobehavioral Reviews*, *37*, 2608–2620.

Helton, W. S. (2009). Impulsive responding and the sustained attention to response task. *Journal of Clinical and Experimental Neuropsychology*, *31*, 39–47.

Hommel, B. (2011). The Simon effect as tool and heuristic. *Acta Psychologica*, *136*, 189–202.

Huster, R. J., Plis, S. M., & Calhoun, V. D. (2015). Group-level component analyses of EEG: Validation and evaluation. *Frontiers in Neuroscience*, *9*, 254.

Keye, D., Wilhelm, O., Oberauer, K., & Stürmer, B. (2013). Individual differences in response conflict adaptations. *Frontiers in Psychology*, *4*, 947.

Kornblum, S., Hasbroucq, T., & Osman, A. (1990). Dimensional overlap: Cognitive basis for stimulus-response compatibility–a model and taxonomy. *Psychological Review*, *97*, 253–270.

Logan, G. D., Cowan, W. B., & Davis, K. A. (1984). On the ability to inhibit simple and choice reaction time responses: A model and a method. *Journal of Experimental Psychology: Human Perception & Performance*, *10*, 276–291.

Logan, G. D., Van Zandt, T., Verbruggen, F., & Wagenmakers, E.-J. (2014). On the ability to inhibit thought and action: General and special theories of an act of control. *Psychological Review*, *121*, 66–95.

Marco-Pallarés, J., Grau, C., & Ruffini, G. (2005). Combined ICA-LORETA analysis of mismatch negativity. *NeuroImage*, *25*, 471–477.

Masson, M. E. J. (2011). A tutorial on a practical Bayesian alternative to null-hypothesis significance testing. *Behavior Research Methods*, *43*, 679–690.

McVay, J. C., & Kane, M. J. (2009). Conducting the train of thought: Working memory capacity, goal neglect, and mind wandering in an executive-control task. *Journal of Experimental Psychology: Learning, Memory, and Cognition*, *35*, 196–204.

Mostofsky, S. H., & Simmonds, D. J. (2008). Response inhibition and response selection: Two sides of the same coin. *Journal of Cognitive Neuroscience*, *20*, 751–761.

Mückschel, M., Chmielewski, W., Ziemssen, T., & Beste, C. (2017a). The norepinephrine system shows information-content specific properties during cognitive control – Evidence from EEG and pupillary responses. *NeuroImage*, *149*, 44–52.

Mückschel, M., Dippel, G., & Beste, C. (2017b). Distinguishing stimulus and response codes in theta oscillations in prefrontal areas during inhibitory control of automated responses. *Human Brain Mapping*.

Mückschel, M., Dippel, G., & Beste, C. (2017c). Distinguishing stimulus and response codes in theta oscillations in prefrontal areas during inhibitory control of automated responses. *Human Brain Mapping*, *38*, 5681–5690.

Mückschel, M., Stock, A.-K., & Beste, C. (2014). Psychophysiological mechanisms of interindividual differences in goal activation modes during action cascading. *Cerebral Cortex (New York, N.Y.: 1991)*, *24*, 2120–2129.

Mückschel, M., Stock, A.-K., Dippel, G., Chmielewski, W., & Beste, C. (2016). Interacting sources of interference during sensorimotor integration processes. *NeuroImage*, *125*, 342–349.

Nieuwenhuis, S., Yeung, N., & Cohen, J. D. (2004). Stimulus modality, perceptual overlap, and the go/no-go N2. *Psychophysiology*, *41*, 157–160.

Nunez, P. L., & Pilgreen, K. L. (1991). The spline-Laplacian in clinical neurophysiology: A method to improve EEG spatial resolution. *Journal of Clinical Neurophysiology*, *8*, 397–413.

Nunez, P. L., Srinivasan, R., Westdorp, A. F., Wijesinghe, R. S., Tucker, D. M., Silberstein, R. B., & Cadusch, P. J. (1997). EEG coherency. I: Statistics, reference electrode, volume conduction, Laplacians, cortical imaging, and interpretation at multiple scales. *Electroencephalography and Clinical Neurophysiology*, *103*, 499–515.

Ocklenburg, S., Güntürkün, O., & Beste, C. (2011). Lateralized neural mechanisms underlying the modulation of response inhibition processes. *NeuroImage*, *55*, 1771–1778.

Ouyang, G., Herzmann, G., Zhou, C., & Sommer, W. (2011). Residue iteration decomposition (RIDE): A new method to separate ERP components on the basis of latency variability in single trials. *Psychophysiology*, *48*, 1631–1647.

Ouyang, G., Hildebrandt, A., Sommer, W., & Zhou, C. (2017). Exploiting the intra-subject latency variability from single-trial event-related potentials in the P3 time range: A review and comparative evaluation of methods. *Neuroscience and Biobehavioral Reviews*, *75*, 1–21.

Ouyang, G., Schacht, A., Zhou, C., & Sommer, W. (2013). Overcoming limitations of the ERP method with Residue Iteration Decomposition (RIDE): A demonstration in go/no-go experiments. *Psychophysiology*, *50*, 253–265.

Ouyang, G., Sommer, W., & Zhou, C. (2015a). Updating and validating a new framework for restoring and analyzing latency-variable ERP components from single trials with residue iteration decomposition (RIDE). *Psychophysiology*, *52*, 839–856.

Ouyang, G., Sommer, W., & Zhou, C. (2015b). A toolbox for residue iteration decomposition (RIDE)–A method for the decomposition, reconstruction, and single trial analysis of event related potentials. *Journal of Neuroscience Methods*, *250*, 7–21.

Pascual-Marqui, R. D. (2002). Standardized low-resolution brain electromagnetic tomography (sLORETA): Technical details. *Methods and Findings in Experimental and Clinical Pharmacology*, *24* Suppl D, 5–12.

Ridderinkhof, K. R., van den Wildenberg, W. P. M., Segalowitz, S. J., & Carter, C. S. (2004). Neurocognitive mechanisms of cognitive control: The role of prefrontal cortex in action selection, response inhibition, performance monitoring, and reward-based learning. *Brain and Cognition*, *56*, 129–140.

Rushworth, M. F., Paus, T., & Sipila, P. K. (2001). Attention systems and the organization of the human parietal cortex. *The Journal of Neuroscience: The Official Journal of the Society for Neuroscience*, *21*, 5262–5271.

Schiff, S., Bardi, L., Basso, D., & Mapelli, D. (2011). Timing spatial conflict within the parietal cortex: A TMS study. *Journal of Cognitive Neuroscience*, *23*, 3998–4007.

Sekihara, K., Sahani, M., & Nagarajan, S. S. (2005). Localization bias and spatial resolution of adaptive and non-adaptive spatial filters for MEG source reconstruction. *NeuroImage*, *25*, 1056–1067.

Stock, A.-K., Gohil, K., Huster, R. J., & Beste, C. (2017). On the effects of multimodal information integration in multitasking. *Scientific Reports*, *7*, 4927.

Takeichi, H., Koyama, S., Terao, A., Takeuchi, F., Toyosawa, Y., & Murohashi, H. (2010). Comprehension of degraded speech sounds with m-sequence modulation: An fMRI study. *NeuroImage*, *49*, 2697–2706.

van Veen, V., & Carter, C. S. (2002). The anterior cingulate as a conflict monitor: fMRI and ERP studies. *Physiology &Amp; Behavior*, *77*, 477–482.

Verleger, R., Metzner, M. F., Ouyang, G., Śmigasiewicz, K., & Zhou, C. (2014). Testing the stimulus-to-response bridging function of the oddball-P3 by delayed response signals and residue iteration decomposition (RIDE). *NeuroImage*, *100*, 271–280.

Verleger, R., Siller, B., Ouyang, G., & Śmigasiewicz, K. (2017). Effects on P3 of spreading targets and response prompts apart. *Biological Psychology*, *126*, 1–11.

Wagenmakers, E.-J. (2007). A practical solution to the pervasive problems of p values. *Psychonomic Bulletin &Amp; Review*, *14*, 779–804.

Wolff, N., Mückschel, M., & Beste, C. (2017). Neural mechanisms and functional neuroanatomical networks during memory and cue-based task switching as revealed by residue iteration decomposition (RIDE) based source localization. *Brain Structure and Function*.

SUPPORTING INFORMATION

Additional Supporting Information may be found online in the supporting information tab for this article.

How to cite this article: Chmielewski WX, Mückschel M, Beste C. Response selection codes in neurophysiological data predict conjoint effects of controlled and automatic processes during response inhibition. *Hum Brain Mapp*. 2018;39:1839–1849. https://doi.org/10.1002/hbm.23974